

Original Article

The effect of the surgical microscope on the outcome of root scaling

Haiqing Liao¹, Huihui Zhang^{1,2}, Junbo Xiang^{1,2}, Guanting Chen^{1,2}, Zhengguo Cao^{1,2}

¹The State Key Laboratory Breeding Base of Basic Science of Stomatology (Hubei-MOST) & Key Laboratory of Oral Biomedicine Ministry of Education, School & Hospital of Stomatology, Wuhan University, Luoyu Road, Wuhan 430079, China; ²Department of Periodontology, School & Hospital of Stomatology, Wuhan University, Luoyu Road, Wuhan 430079, China

Received June 5, 2020; Accepted October 10, 2020; Epub November 15, 2020; Published November 30, 2020

Abstract: The benefits of using a surgical microscope in periodontal therapy were mainly based on subjective statements made by patients or periodontists. We aimed to provide laboratory evidence for the advantages of using a surgical microscope during root scaling on periodontitis teeth. In the present study, the extracted teeth were categorized into four groups: normal teeth (normal control [NC] group), untreated periodontitis teeth (periodontitis control [PC] group), root surface scaled without magnification (macro group), and root surface instrumented with a microscope (micro group). To analyze both the mechanical and biological properties of the root surfaces, we performed nanoindentation in addition to the traditional methods. We found that by using a surgical microscope, we improved the clearance of bacterial deposits and calculi on periodontitis root surfaces. Nanoindentation results revealed that the nanotopography pattern, elastic modulus, and nanohardness of the root surface in the micro group were closest to those in the NC group. The immunofluorescence assay and cell proliferation analyses revealed improved morphology and enhanced adhesion and proliferation of periodontal ligament cells on the root surface in the micro group compared with the macro group. After instrumentation, the expression levels of interleukin-6 and interleukin-8 decreased when compared with the PC group. Our results demonstrated that surgical microscope application could improve the outcomes of periodontal treatment, implying that a surgical microscope can be a powerful tool for periodontists to seek accurate clinical periodontal performance and gain better biocompatibility of the treated root surfaces.

Keywords: Periodontitis, surgical microscope, biomechanics, nanoindentation

Introduction

Periodontitis is a common inflammatory disease, which is initiated and sustained by periodontal pathogens and their cell-associated and extracellular virulence factors [1, 2]. Contemporary periodontal therapy generally aims at the removal of bacterial deposits (calculus and endotoxin) and restoration of tooth aesthetics and function, which is performed with minimal trauma and discomfort using magnification systems and periodontal microsurgery in addition to conventional technology [3]. However, the benefits of using a surgical microscope in periodontal therapy were mainly based on subjective statements made by patients or periodontists.

In the past decade, using magnification systems and periodontal microsurgery was a part

of minimally invasive surgery in dentistry. There are numerous advantages of using a surgical microscope. For example, practitioners can magnify and illuminate the tooth to be treated, improving the diagnosis and technical accuracy. Although a surgical microscope is widely used in endodontics [4-7], its application in periodontics is currently under active research. Using a microscope in mucogingival periodontal surgery was practiced only by few practitioners, and the use was mainly limited to case report [8-11]. Hegde and Sitbon pointed out that despite the apparent advantages, the actual benefits of the microsurgical approach over conventional approaches have not been estimated in scientific research [3, 12].

Successful periodontal treatment should completely remove bacterial deposits and calculi without exerting any iatrogenic effects [13]. In

Surgical microscope-enhanced root scaling

this regard, to evaluate the advantages of using a surgical microscope during periodontal therapy, we assessed residual calculi and other parameters on the extracted root surfaces after scaling under a microscope and without magnification. Previous studies mainly used traditional methods of the scanning electron microscope (SEM) and surface profilometry and ranked such characteristics by a subjective judgment to determine the characteristics of the tooth root surface [13-17]. The methods cannot precisely elucidate the detailed characteristics of the root surface but can evaluate few biological properties. Thus, the development of more sensitive and detailed approaches is needed.

In recent years, the development and application of scanning probe microscope has accelerated the progress of nanotechnology. It becomes an important supplement to SEM by making sensitive information on the materials available and allowing an understanding of the properties of materials at the nanoscale level. In the present study, in addition to traditional methods, we performed nanoindentation to accurately investigate the biomechanical properties and nanotopography changes on the periodontitis root surfaces at the nanoscale. To determine their cellular reaction after instrumentation, we also cultured periodontal ligament cells (PDLCs) on the root surface.

We aimed to determine whether the application of a surgical microscope could help eliminate the bacterial deposits (calculus and endotoxin) thoroughly on the root surface *in vitro* and to provide new insights into the accurate measurement of the mechanical properties of the root surface under physiological and pathological conditions by nanoindentation technique.

Materials and methods

Sample preparation

The participants of this study were patients aged 30-50 years with advanced chronic periodontitis, with molars scheduled for extraction, and had no periodontal treatment for at least 5 years. The extracted molars were all characterized as hopeless [18, 19] and were randomly assigned into three groups: untreated periodontitis teeth (periodontitis control [PC] group), root surface scaled without mag-

nification (macro group), and root surface instrumented with a microscope (micro group). The impacted third molars were collected from healthy participants and designated as the normal control (NC) group. The use of human teeth was reviewed and approved by the local ethics committee at the School of Stomatology, Wuhan University, and written consent was obtained from each patient. All the selected teeth had no caries and had not received treatments before. After extraction, the upper two-thirds of the selected experimental root surface was divided into a rectangular area of interest (AOI).

The teeth in the macro group were scaled without magnification, and those in the micro group were scaled under the microscope (magnification $\times 10$) (Zumax OMS2380; Suzhou, China). Moreover, all teeth in these two experimental groups were scaled with a magnetostrictive ultrasonic device (Cavitron Bobcat Pro.; Dentsply, York, PA, USA) and were set at a frequency of approximately 25 kHz with P-10 subgingival tip. To model the clinical periodontal surgery, we held the teeth in the occlusal plane location of the patient. A well-trained operator performed root surface debridement of each tooth until the root surfaces were visually cleaned. Two investigators evaluated the specimens under the same conditions. Specimens were prepared into rectangular slices (3 mm \times 2 mm) with a 1-mm thickness within the AOI for the following assays.

Microscopy

Both the cell-free specimens and specimens with cementoblasts or PDLCs cultured on the surfaces were fixed in a 2.5% glutaraldehyde solution at 4°C overnight. The specimens were then soaked in PBS, dehydrated in an alcohol gradient, gold-sputtered, and observed under an SEM (Quanta SEM; Thermo Fisher Scientific, Waltham, MA, USA).

The adhesion and growth of PDLCs on the root surface were analyzed using confocal laser scanning microscopy (Olympus FluoView FV1200; Olympus, Melville, NY, USA). The cells were seeded on the sterile specimens (3000 cells per specimen) and grew for 24 h in basal medium. The samples were washed three times with PBS, fixed in 4% paraformaldehyde for 15 min, and rewashed three times. The

Surgical microscope-enhanced root scaling

cells were permeabilized using 0.1% Triton X-100 for 5 min at 37°C and blocked by premium-quality normal goat serum for 30 min at 37°C. After blocking, the F-actin cytoskeleton of cells was stained with rhodamine phalloidin for 30 min at 37°C, and the nuclei were stained with DAPI for 5 min at room temperature. The confocal images were obtained immediately after the staining. Images of the distribution of cells on the root surface (Z-stack) were obtained.

Nanoindentation testing

The specimens were embedded in epoxy resin with the root surface up, exposed and paralleled to the bottom face, and then stored in PBS at low temperature. We performed the nanoindentation tests by using a nanoindenter (Hysitron TI950; Hysitron Inc., Minneapolis, MN, USA) equipped with a diamond Berkovich three-sided pyramid probe in load control with arising time of 5 s to a maximum load of 1000 μN and unloading rate of 200 $\mu\text{N/s}$. Before the tests, the specimens were air-dried and restored at room temperature for 30 min. Indents were completed in the longitudinal direction on the root surfaces. An array of 36 indents was performed at one position (40 μm \times 40 μm area), and three replicate positions were made available in the identified AOIs of each specimen. Experimental data from all tests were analyzed by Hysitron TriboScan software (Hysitron Inc.).

Cell culturing

Premolars with healthy PDL tissue were collected from donors aged 12-20 years from the School of Stomatology of Wuhan University. Briefly, periodontal ligament tissues were separated from the middle third of the root surface and cut into small pieces. The tissue blocks were digested with 2 mg/mL collagenase type I (SCR103; Sigma-Aldrich, St. Louis, MO, USA) for 110 min at 37°C. To terminate the reaction, we used α -MEM (HyClone, Logan, UT, USA) containing 10% FBS (Gibco, Grand Island, NY, USA). After being centrifuged and resuspended, the tissue explants and cell suspension were transferred and plated into a primary culture dish with the basal medium. The tissues were incubated in a humidified atmosphere of 5% CO_2 at 37°C until cells grew out from the tissue patch and reached 80% confluence. The tissues were then subcultured.

The immortalized mouse cementoblast cell line (OCCM-30) was cultured in Dulbecco's Modified Eagle's Medium (Hyclone) containing 10% FBS (Gibco) in 5% CO_2 at 37°C.

Cell proliferation

Tooth samples were immersed in 75% ethanol for 1 h and exposed to ultraviolet light for 30 min for sterilization. PDLs were plated in 24-well plates, in which the sterile tooth sample was pre-placed, at a concentration of 1×10^5 cells/well, and cultured in basal medium. The cells grew for 6 h to attach on the root surface and were transferred to the 96-well plates. To determine cell proliferation each day of the 4-day culture period, we used Cell Counting Kit-8 (CCK-8) (Dojindo, Kumamoto, Japan) to record the absorbance at 450-nm wavelength.

Enzyme-linked immunosorbent assay (ELISA)

Tooth samples were sterilized by steam sterilization. PDLs were seeded onto the samples (using the method in the Cell Proliferation section) and incubated for 24 h. The concentrations of interleukin-6 (IL-6) and interleukin-8 (IL-8) in the supernatant were determined by an ELISA kit (Boster Biological Technology Ltd., Pleasanton, CA, USA) according to the manufacturer's instructions. The plates were read using ELISA reader (PowerWave XS2; BioTek, Winooski, VT, USA) at 450-nm wavelength.

Statistical analysis

All data were expressed as means \pm standard deviation (SD). Differences among groups were measured with GraphPad Prism 5 (GraphPad Software Inc., San Diego, CA, USA) using a one-way analysis of the variance and Tukey's multiple comparison tests. The Student's *t*-test was used to compare the results between the two groups. Statistical difference was considered at $P < 0.05$ and $P < 0.01$.

Results

Evaluation of stained deposits

To observe the residual calculi in different experimental groups, we conducted a paired experimental design after treatment. The mean percentages of the stained calculus in each experimental group after instrumentation were 17.0% (macro group) and 9.9% (micro group)

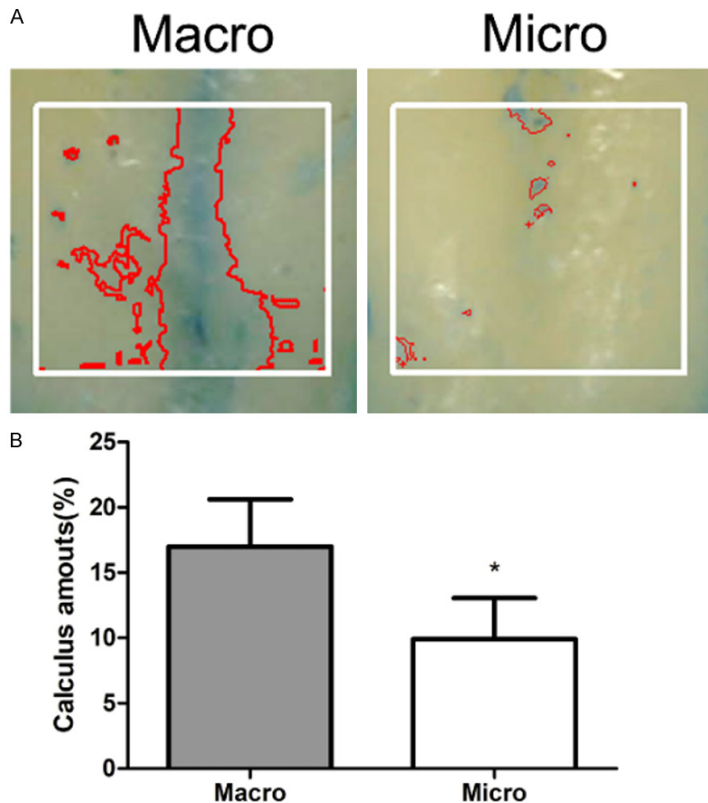


Figure 1. Residual calculi on the root surface. A. Digital planimetric root surface analysis of AOI after staining with methylene blue. B. Mean calculus amounts for each group after instrumentation. Macro, roots treated without magnification. Micro, roots treated under surgical microscope. Data were expressed as mean \pm SD from at least three independent experiments. * $P < 0.05$ (Student's *t*-test).

(**Figure 1B**). A statistically significant difference at $P < 0.01$ was observed between the macro and micro groups.

SEM

Figure 2 shows the root surface of healthy and periodontically-compromised teeth before and after instrumentation. The healthy root surface (**Figure 2A**) was relatively regular and had a dome-shaped cementum structure covering on it. The residual collagen fiber bundle was firmly attached to the cementum. The periodontitis root surface had a highly irregular pattern with a ballast-like structure (**Figure 2B**). After scaling, the root surfaces became considerably flatter both in the macro group (**Figure 2C**) and the micro group (**Figure 2D**). This finding indicates the loss of the normal structure, which might be the cementum. Moreover, the root surface in the macro group seemed to be covered with a thicker smear layer; specimens in the micro group had a relatively cleaner surface.

Nanoindentation

Figure 3A shows the representative indentation array script of a $40 \mu\text{m} \times 40 \mu\text{m}$ area of each group. The corresponding nano-3D plots revealed the different surface morphologies of specimens in different groups. The NC group had a relatively regular structure and considerably smaller structural units (**Figure 3Bb1**) than the PC group (**Figure 3Bb2**). Loss of the normal surface structure, exposure of the inner structure, and formation of groove defects were observed in the macro group (**Figure 3Bb3**). However, the root surface structure instrumented under the microscope remained similar to that in the NC group (**Figure 3Bb4**).

The distributions of modulus and nanohardness values in the four groups are respectively shown in **Figure 4A**, **4B**. Among the four groups, the reduced modulus and nanohardness of the root surface were the highest in the PC group (E_r : 20.03 GPa; H : 0.4982 GPa) and the lowest in the NC group (E_r : 7.095 GPa; H : 0.1625 GPa).

The macro group had a larger 95% CI of reduced modulus and nanohardness (E_r : mean 15.21 GPa, 95% CI: 13.16-17.27 GPa; H : mean 0.3317 GPa, 95% CI: 0.2455-0.4179 GPa), than the Macro group (E_r : mean 15.21 GPa, 95% CI: 13.16-17.27 GPa; H : mean 0.2080 GPa, 95% CI: 0.1933-0.2227 GPa). However, no statistically significant differences were observed between the two groups. Furthermore, the distributions of scatters in the micro group appeared similar to those in the NC group.

Cell morphology on the root surface

Figure 5A shows the confocal microscope images of PDLCs cultured on the root surface in each group. From the images of F-actin, it could be observed clearly that PDLCs adhered and stretched best on the root surface in the NC group, had extended branched projections and had most dimensional space structures compared with the cells in the other groups. By contrast, PDLCs on the root surface in the PC group manifested marked morphological

Surgical microscope-enhanced root scaling

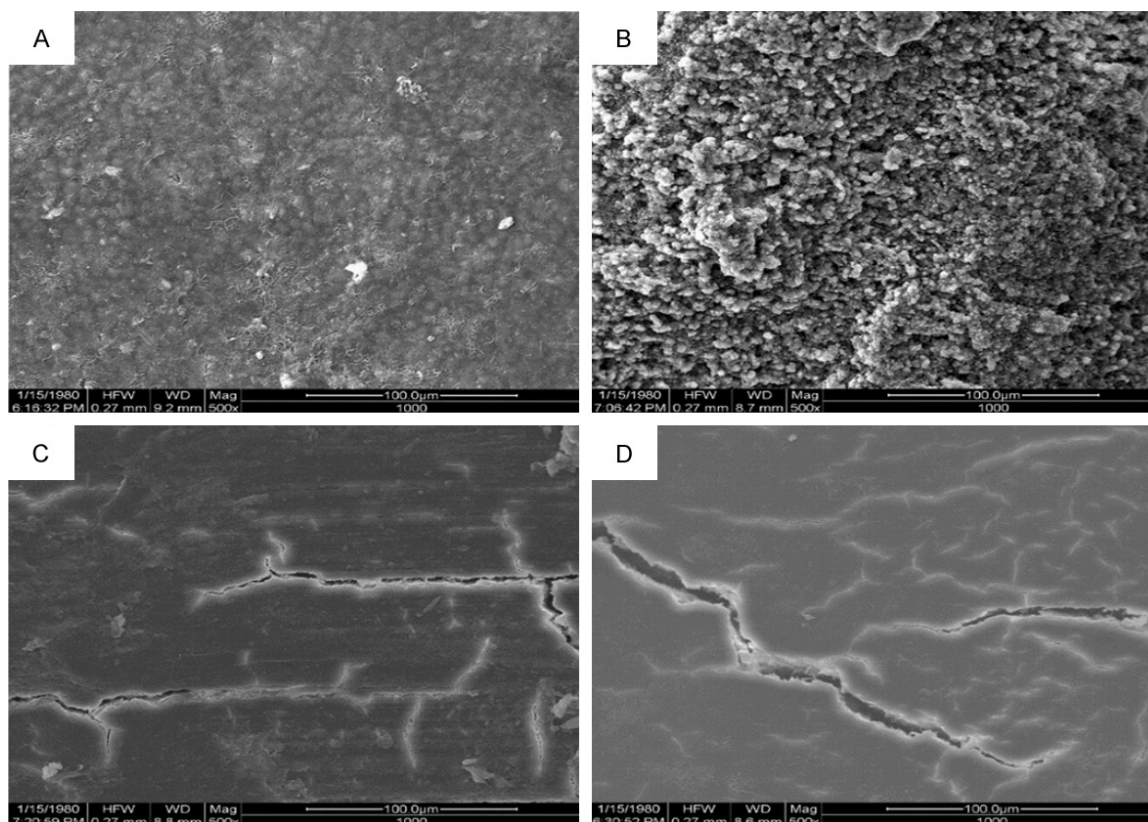


Figure 2. Representative SEM morphology of the root surfaces (original magnification $\times 500$). A. NC group (healthy root surface) with a regular dome-shaped cementum structure. B. PC group (untreated periodontitis root surface) with a highly irregular pattern with a ballast-like structure. C. Macro group (roots treated without magnification) with a thicker smear layer. D. Micro group (roots treated under a surgical microscope) with a clean and flat root surface. The scale bar is 100 μm .

changes. Shrinkage and detachment of PDLCs were observed. Meanwhile, moderate cell morphological changes were found in the micro group as compared with the flattened and shrank cells on the root surface in the macro group.

Representative SEM images of cells cultured on root surfaces showed that the cementoblasts firmly gripped the dome-shaped cementum structure on the root surface with its cellular protrusions (**Figure 5B**). It also suggested that the regular dome-shaped cementum structure was important to cell adhesion. The SEM images also showed the morphology of PDLCs with cellular protrusions extending to adhere to the fibers on the root surface (**Figure 5C**).

Cell proliferation

The time-related proliferation of PDLCs was evaluated by CCK-8 assay (**Figure 6**). After cul-

turing for 2 days, the proliferation of PDLCs on the root surface in the micro group was statistically higher ($P < 0.05$) than that in the PC group and was the highest among all groups. This trend continued for 4 days. As the culture time was extended to day 3 and day 4, the speed of cell proliferation in the macro group became slower than that in the NC group, although it was almost the same in day 1 and day 2. The number of cells in the PC group remained to be the lowest during culturing.

IL-6 and IL-8 secretions

The secretions of IL-6 and IL-8, markers of inflammation, were quantified by ELISA (**Figure 7**). Among the four groups, the results demonstrated that both the expression levels of IL-6 and IL-8 were lowest in the NC group and highest in the PC group. After instrumentation, the expression levels of IL-6 and IL-8 in macro and micro groups decreased remarkably when

Surgical microscope-enhanced root scaling

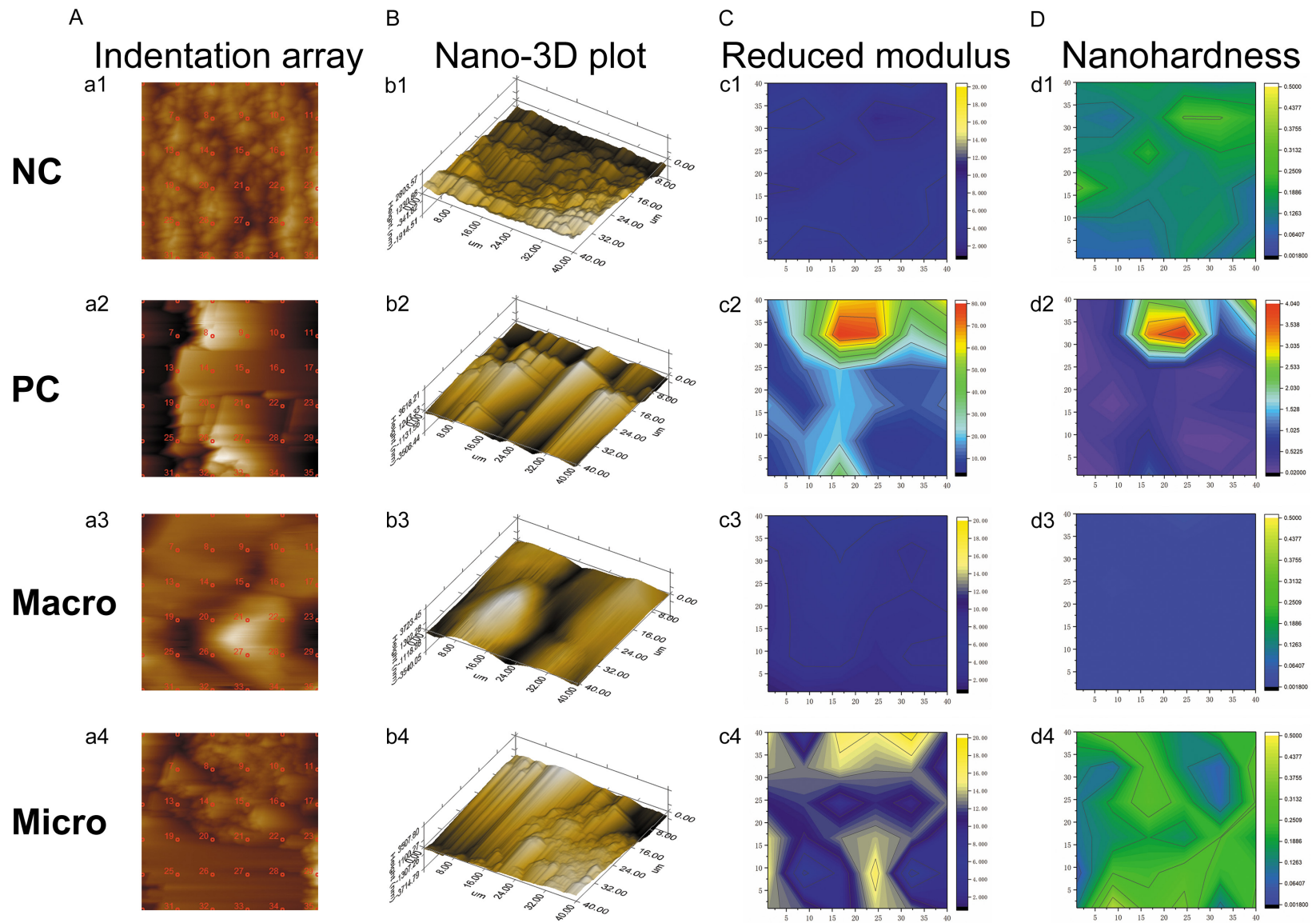


Figure 3. Representative nanoindentation profile at one position of the root surface in each group. A. Indentation array script of a 40 $\mu\text{m} \times 40 \mu\text{m}$ area. B. Corresponding nano-3D plot. C. Corresponding contour map of reduced modulus. D. Corresponding contour map of nanohardness.

Surgical microscope-enhanced root scaling

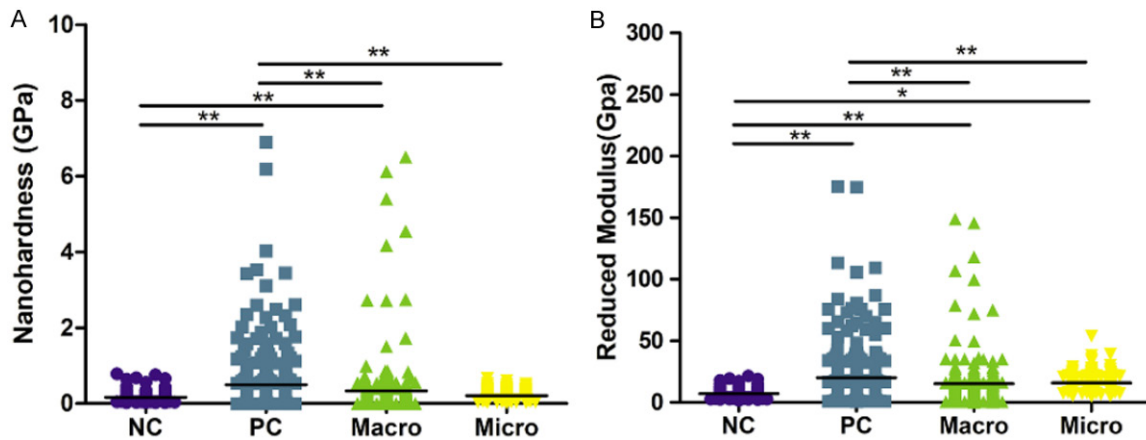


Figure 4. Overall reduced modulus (E_r) and nanohardness profiles of the tooth root surfaces in each group. A. Reduced moduli (E_r) of the tooth root surfaces in four groups. B. Nanohardnesses of the tooth root surfaces in four groups. A statistically significant difference was observed at $*P < 0.05$ and $**P < 0.01$ (one-way ANOVA, followed by Tukey's multiple comparison tests).

compared with those in the PC group. We could observe that the expression levels of IL-6 and IL-8 in the micro group were a bit lower than those in the macro group, although the differences were not significant.

Discussion

Surgical microscope has been widely used in many fields; however, its popularity and application in periodontics still lack enough scientific studies. In this study, to evaluate the benefits of using a surgical microscope in periodontal therapy, we accurately investigated the biomechanical properties, nanotopography changes, and biological properties of the root surfaces by performing nanoindentation in addition to traditional methods.

The removal of plaque and calculus is an indicator of successful periodontal treatment. The amount of residual deposits after scaling was evaluated through stained deposits (**Figure 1**) and SEM analysis (**Figure 2**). With the use of a surgical microscope, the calculus coverage decreased noticeably after instrumentation ($P < 0.01$). It is suggested that the broadened version helped in removing the calculus effectively.

Our SEM examinations on the root surface patterns confirmed the findings from previous studies [13-16]. Our results and the work by Kawashima et al. [13] found that a relatively normal root surface displayed dome-shaped

cementum structure. Busslinger found a smear layer that covered the root surfaces and gouges probably because of the instrument tips after conventional scaling [16]. In the present study, the smear layer, grooves, defects, and linear injuries were also found after instrumentation. They were more pronounced in the macro group than in the micro group. Also, our SEM morphology illustrated the robust residual collagens that are attached to the normal root surface (**Figure 2A**). Geiger reported that many extracellular matrix proteins could be recognized by integrin receptors on the cell membrane; such proteins may transduce mechanochemical cues from the environment to the cell [20]. Collagen fiber alignment and density could modulate cell migration [21-23]. Our SEM images of cells cultured on root surfaces (**Figure 5B, 5C**) also demonstrated that regular dome-shaped cementum structure and fibers on the root surface were crucial for cell adhesion. Accordingly, keeping the structure as intact as possible during periodontal treatment is important to the cells in response to the root surface and tissue regeneration.

To evaluate the effectiveness of microscope-enhanced scaling, we also investigated the mechanical properties of the root surface. Nanoindentation provided new insights on the mechanical properties and topography of the periodontitis root surface at nanoscale. Regarding mechanical properties, nanoindentation at one representative injured position (**Figure 3Aa3**) revealed that the reduced modu-

Surgical microscope-enhanced root scaling

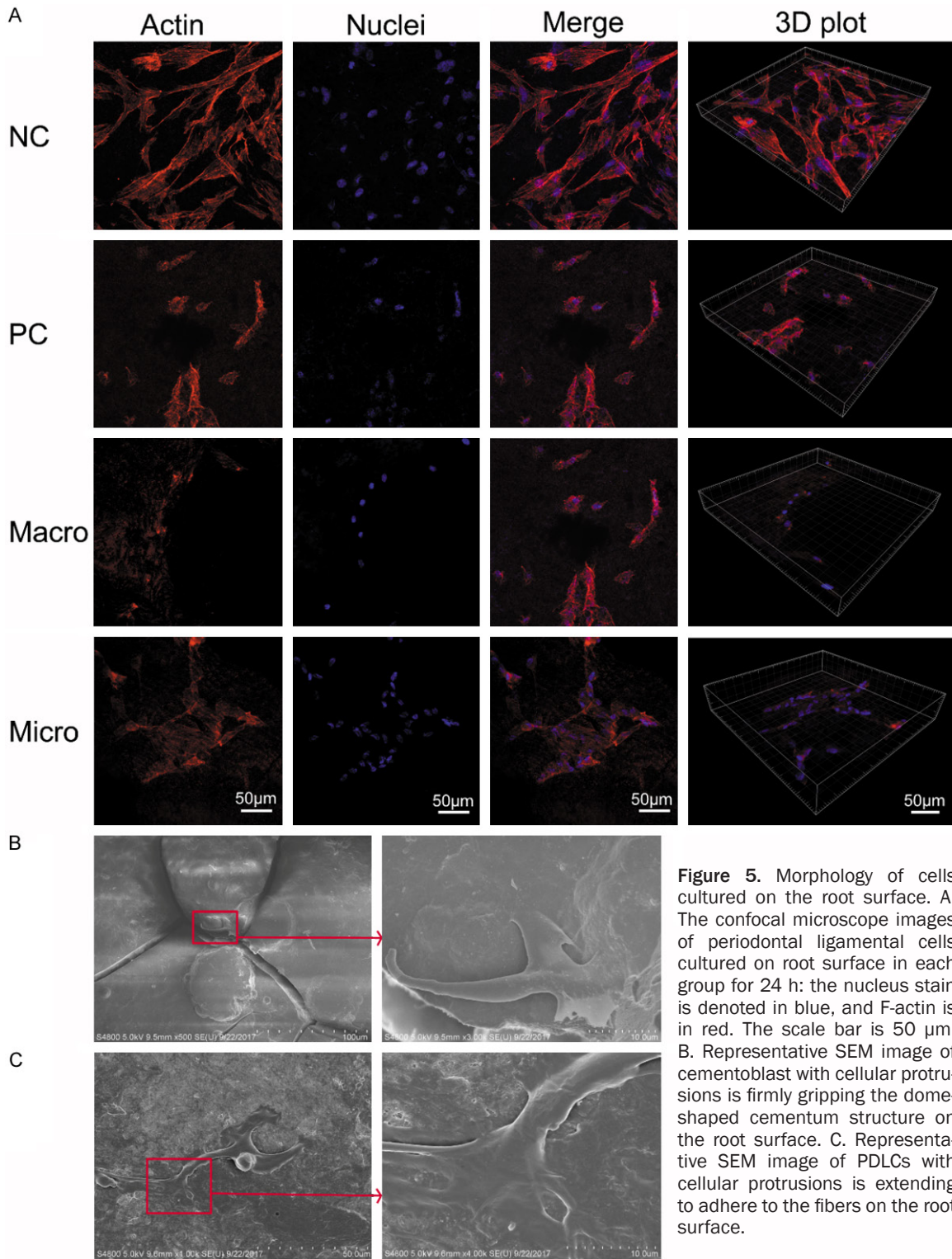


Figure 5. Morphology of cells cultured on the root surface. A. The confocal microscope images of periodontal ligamental cells cultured on root surface in each group for 24 h: the nucleus stain is denoted in blue, and F-actin is in red. The scale bar is 50 μ m. B. Representative SEM image of cementoblast with cellular protrusions is firmly gripping the dome-shaped cementum structure on the root surface. C. Representative SEM image of PDLCs with cellular protrusions is extending to adhere to the fibers on the root surface.

lus and nanohardness decreased after the injury when compared with those in the other groups (**Figure 3C, 3D**). On the basis of a previous study, tooth root has multi-layer structures with a natural interface between cemen-

tum and dentin, and the hardness exhibits a gradual transition from the cementum to dentin [24]. Thus, the decreased value of reduced modulus and nanohardness on the root surface might imply the loss of cementum and

Surgical microscope-enhanced root scaling

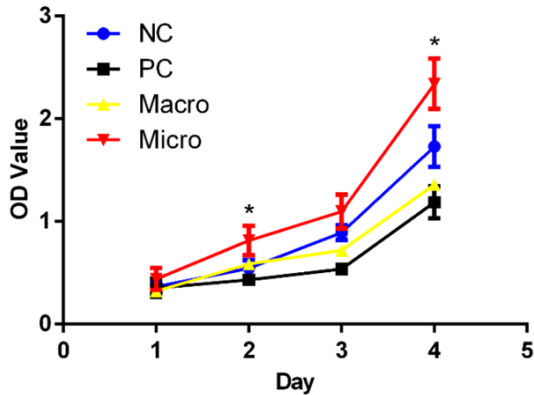


Figure 6. The proliferation of PDLCs cultured on the root surface of each group for 1-4 days. Data were expressed as mean \pm SD from at least three independent experiments. Compared with the PC group at the same time, * $P < 0.05$ (one-way ANOVA, followed by Tukey's multiple comparison tests).

exposure to the internal structure. Also, the nano-3D plot (**Figure 3Bb3**) provided an intuitive and convenient approach to observe such damage on the periodontitis root surface. On the other hand, the considerably higher values of reduced modulus and nanohardness in the PC group indicated that the calculus has distinct mechanical properties to normal root surface tissues. Moreover, the distribution patterns of the reduced modulus and nanohardness values in the micro group were closer to those in the NC group but considerably varied from those in the macro group. We should note that changes in tooth biomechanics can, in turn, alter the entire bone-tooth complex including cell's behavior inside [25]. Super elastic properties and hardness are essential in medical applications because of the large strains and deformation at which the tooth is subjected [26]. Accordingly, accurate measurements of the mechanical properties of the tooth have great instruction significance for oral clinical performance. Our results suggested that deviations from reduced modulus and nanohardness values of normal tooth surface might imply residual calculi and the destruction of the root surface after scaling.

The results of nanoindentation provide knowledge about the physical topographical features both of the periodontitis and normal root surface at nanoscale. The nano-3D plots display differences in nanotopography among the four groups. The normal root surface had a relatively regular structure and considerably smaller

structural units than those in the PC group. The untreated periodontitis root surface had a shale-like structure with bigger units, plane faces, sharper edges and corners (**Figure 3Bb2**). Nanotopography alone could remarkably influence various kinds of cells [27-31]. In the present study, the morphology of PDLCs varied on different root surfaces (**Figure 6**); PDLCs adhered and stretched best on the root surface in the NC group. However, PDLCs were seriously shrunk and detached in the PC group. There were moderate cell morphological changes observed in the micro group compared with the flattened and shrank cells on the root surface in the macro group. This finding may suggest that more normal surface structures were preserved during the treatment under the microscope compared with those instrumented without magnification.

Cell proliferation indicates the residual amount of microbial toxin and biocompatibility of the root surface. In our study, to evaluate root surface properties, we selected PDLCs because these cells contained stem/progenitor cells and possessed the high potential for regeneration of the bone, cementum, and PDL upon *in vivo* transplantation [32-34]. Interestingly, after 4 days of culture, the proliferation speed of PDLCs in the micro group was the fastest among the four groups, surpassing even that in the NC group. PDLCs play a key role in periodontal tissue regeneration; thus, enhanced PDLC proliferation indicated that surgical microscopy might contribute to reducing microbial toxin and improving periodontal tissue regeneration.

Reducing inflammation is an important goal of periodontal treatment. To confirm the influence of different root conditioning methods on reducing inflammation, we performed ELISA assay to measure the IL-6 and IL-8 expressions of PDLCs. Among the four groups, the results revealed that both the IL-6 and IL-8 concentrations were the lowest in the NC group and the highest in the PC group (**Figure 7**). After instrumentation, the expression levels of IL-6 and IL-8 in macro and micro groups decreased remarkably when compared with those in the PC group. From the results, we found that scaling under the microscope helped reduce the IL-6 and IL-8 secretions a bit when compared with the group without magnification. In reducing inflammation, Rethman reported that it is

Surgical microscope-enhanced root scaling

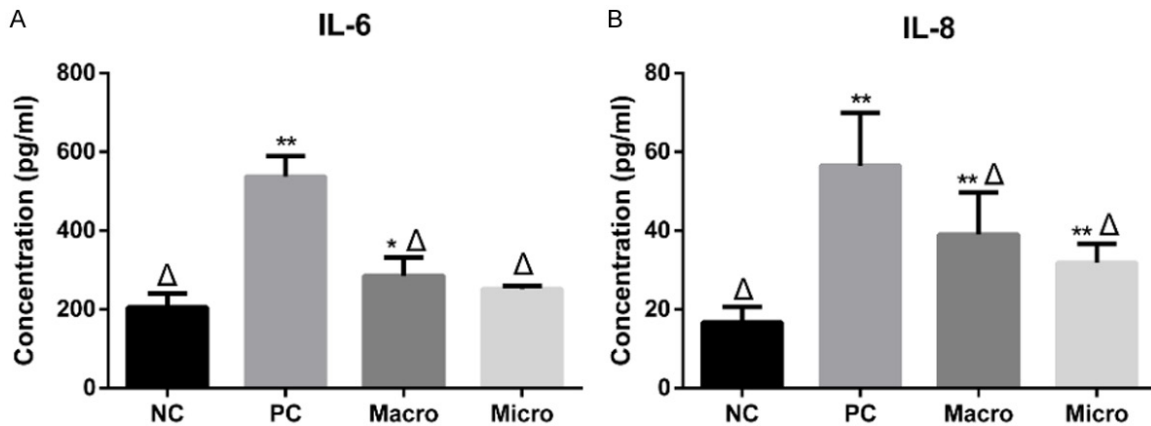


Figure 7. Pro-inflammatory cytokines expressed by PDLs on different root surfaces. (A) IL-6 and (B) IL-8 expressed by PDLs on different root surfaces were determined by ELISA. Data were expressed as mean \pm SD from at least three independent experiments. Compared with the NC group, * $P < 0.05$ and ** $P < 0.01$; compared with the PC group, $\Delta P < 0.01$ (one-way ANOVA, followed by Tukey's multiple comparison tests).

difficult to achieve at the deep probing depths by using blind methods [35]. Similarly, Lindhe et al. found that areas with unresolved inflammation and deep residual probing depths caused by incomplete debridement often progress over time [36]. Therefore, we suggest a thorough removal of residual calculus on the root surface without injuring the normal structure via a more precise and magnified vision acquired using a surgical microscope.

The surgical microscope can assist the periodontists when performing especially sensitive operations by allowing instant feedback of tiny details. Nevertheless, the anatomical aspect, tooth morphology, deep probing depth, presence of suppuration, and bleeding on probing should reduce the ability of the microscopic view and the operator efficacy. At the initial scaling-surfacing phase, the persistence of dental plaque and calculi on root surfaces could be better removed if done with a flap exposure under microscope magnification. Thus, it is the periodontists' professional judgment on the need for this procedure, depending on the severity and features of the disease [12]. Because the use of a microscope needs extensive training and practice, this factor surely may impact the effects of periodontal treatment as well as the results in this study. Moreover, this *in vitro* study does not replicate equally the subgingival scaling as performed in the patient's mouth. Thus, the randomized clinical trial should be implemented to evaluate the merits of using a surgical microscope in periodontics.

Conclusion

Our study demonstrated that using a surgical microscope during periodontal treatment contributed to reducing bacterial deposits and calculi *in vitro*. It improved the preservation of the normal root surface structure and the cell reaction and had better biomechanical properties. This study also gave new insights into mechanical properties and nanotopography of the tooth root surface by the nanoindentation technique. Even though our study suggests that a surgical microscope might be a powerful tool for accurate clinical performance in periodontics, more clinical studies should be performed to evaluate the merits of a surgical microscope and decide if it should be a standard of care in periodontics.

Acknowledgements

This work was partially supported by the National Natural Science Foundation of China (No. 81870776 and 8140054) and the Youth Science Foundation of Guangxi Medical University (No. GXMUYSF201926).

Disclosure of conflict of interest

None.

Address correspondence to: Zhengguo Cao, Department of Periodontology, School & Hospital of Stomatology, Wuhan University, 237 Luoyu Road, Hongshan District, Wuhan 430079, China. Tel: +86-027-87686212; E-mail: caozhengguo@whu.edu.cn

Surgical microscope-enhanced root scaling

References

- [1] Berezow AB and Darveau RP. Microbial shift and periodontitis. *Periodontol* 2000 2011; 55: 36-47.
- [2] Feghali K and Grenier D. Priming effect of fibronectin fragments on the macrophage inflammatory response: potential contribution to periodontitis. *Inflammation* 2012; 35: 1696-1705.
- [3] Hegde R, Sumanth S and Padhye A. Microscope-enhanced periodontal therapy: a review and report of four cases. *J Contemp Dent Pract* 2009; 10: E088-96.
- [4] Brignardello-Petersen R. Use of a microscope during endodontic treatment seems to have helped locating second mesiobuccal root in maxillary first molars that needed retreatment. *J Am Dent Assoc* 2017; 148: e121.
- [5] Ashwinkumar V, Nandini S and Velmurugan N. Endodontic management of three-canal mandibular lateral incisor using dental operating microscope. *J Dent* 2014; 11: 490.
- [6] Khalighinejad N, Aminoshariae A, Kulild JC, Williams KA, Wang J and Mickel A. The effect of the dental operating microscope on the outcome of nonsurgical root canal treatment: a retrospective case-control study. *J Endod* 2017; 43: 728-732.
- [7] Perrin P, Neuhaus KW and Lussi A. The impact of loupes and microscopes on vision in endodontics. *Int Endod J* 2014; 47: 425-429.
- [8] Cortellini P and Tonetti MS. Microsurgical approach to periodontal regeneration. Initial evaluation in a case cohort. *J Periodontol* 2001; 72: 559-569.
- [9] Cortellini P and Tonetti MS. Clinical performance of a regenerative strategy for intrabony defects: scientific evidence and clinical experience. *J Periodontol* 2005; 76: 341-350.
- [10] Wachtel H, Schenk G, Böhm S, Weng D, Zuhr O and Hürzeler MB. Microsurgical access flap and enamel matrix derivative for the treatment of periodontal intrabony defects: a controlled clinical study. *J Clin Periodontol* 2003; 30: 496-504.
- [11] Burkhardt R and Lang NP. Coverage of localized gingival recessions: comparison of micro and macrosurgical techniques. *J Clin Periodontol* 2005; 32: 287-293.
- [12] Sitbon Y and Attathom T. Minimal intervention dentistry II: part 6. Microscope and microsurgical techniques in periodontics. *Br Dent J* 2014; 216: 503.
- [13] Kawashima H, Sato S, Kishida M and Ito K. A comparison of root surface instrumentation using two piezoelectric ultrasonic scalers and a hand scaler in vivo. *J Periodontol* 2007; 42: 90-95.
- [14] Santos FA, Pochapski MT, Leal PC, Gimenes-Sakima PP and Marcantonio E Jr. Comparative study on the effect of ultrasonic instruments on the root surface in vivo. *Clin Oral Investig* 2008; 12: 143-150.
- [15] Tsurumaki Jdo N, Souto BH, Oliveira GJ, Sampaio JE, Marcantonio Júnior E and Marcantonio RA. Effect of instrumentation using curettes, piezoelectric ultrasonic scaler and Er,Cr:YSGG laser on the morphology and adhesion of blood components on root surfaces: a SEM study. *Braz Dent J* 2011; 22: 185-192.
- [16] Busslinger A, Lampe K, Beuchat M and Lehmann B. A comparative in vitro study of a magnetostrictive and a piezoelectric ultrasonic scaling instrument. *J Clin Periodontol* 2001; 28: 642-649.
- [17] Mittal A, Nichani AS, Venugopal R and Rajani V. The effect of various ultrasonic and hand instruments on the root surfaces of human single rooted teeth: a planimetric and profilometric study. *J Indian Soc Periodontol* 2014; 18: 710-717.
- [18] Machtei EE and Hirsch I. Retention of hopeless teeth: the effect on the adjacent proximal bone following periodontal surgery. *J Periodontol* 2007; 78: 2246-2252.
- [19] Kwok V and Caton JG. Commentary: prognosis revisited: a system for assigning periodontal prognosis. *J Periodontol* 2007; 78: 2063-2071.
- [20] Geiger B, Spatz JP and Bershadsky AD. Environmental sensing through focal adhesions. *Nat Rev Mol Cell Biol* 2009; 10: 21-33.
- [21] Ray A, Slama ZM, Morford RK, Madden SA and Provenzano PP. Enhanced directional migration of cancer stem cells in 3D aligned collagen matrices. *Biophys J* 2017; 112: 1023-1036.
- [22] Fraley SI, Wu PH, He L, Feng Y, Krisnamurthy R, Longmore GD and Wirtz D. Three-dimensional matrix fiber alignment modulates cell migration and MT1-MMP utility by spatially and temporally directing protrusions. *Sci Rep* 2015; 5: 14580.
- [23] Hou Y, Rodriguez LL, Wang J and Schneider IC. Collagen attachment to the substrate controls cell clustering through migration. *Phys Biol* 2014; 11: 056007.
- [24] Ho SP, Balooch M, Marshall SJ and Marshall GW. Local properties of a functionally graded interphase between cementum and dentin. *J Biomed Mater Res A* 2004; 70: 480-489.
- [25] Jang AT, Lin JD, Choi RM, Choi EM, Seto ML, Ryder MI, Gansky SA, Curtis DA and Ho SP. Adaptive properties of human cementum and cementum dentin junction with age. *J Mech Behav Biomed Mater* 2014; 39: 184-196.

Surgical microscope-enhanced root scaling

- [26] Yate L, Coy LE, Gregurec D, Aperador W, Moya SE and Wang G. Nb-C nanocomposite films with enhanced biocompatibility and mechanical properties for hard-tissue implant applications. *Acs Appl Mater Interfaces* 2015; 7: 6351-6358.
- [27] Park S and Im GI. Stem cell responses to nanotopography. *J Biomed Mater Res A* 2015; 103: 1238-1245.
- [28] Yoo J, Noh M, Kim H, Jeon NL, Kim BS and Kim J. Nanogrooved substrate promotes lineage reprogramming of fibroblasts to functional induced dopaminergic neurons. *Biomaterials* 2015; 45: 36-45.
- [29] Saha S, Kumar R, Pramanik K and Biswas A. Interaction of osteoblast -TiO₂ nanotubes in vitro: the combinatorial effect of surface topography and other physico-chemical factors governs the cell fate. *Appl Surf Sci* 2018; 449: 152-165.
- [30] Soares DG, Zhang Z, Mohamed F, Eyster TW, de Souza Costa CA and Ma PX. Simvastatin and nanofibrous poly(l-lactic acid) scaffolds to promote the odontogenic potential of dental pulp cells in an inflammatory environment. *Acta Biomater* 2018; 68: 190-203.
- [31] Lopacinska JM, Gradinaru C, Wierzbicki R, Kobler C, Schmidt MS, Madsen MT, Skolimowski M, Dufva M, Flyvbjerg H and Molhave K. Cell motility, morphology, viability and proliferation in response to nanotopography on silicon black. *Nanoscale* 2012; 4: 3739-3745.
- [32] Seo BM, Miura M, Gronthos S, Bartold PM, Bataouli S, Brahim J, Young M, Robey PG, Wang CY and Shi S. Investigation of multipotent postnatal stem cells from human periodontal ligament. *Lancet* 2004; 364: 149-155.
- [33] Su F, Liu SS, Ma JL, Wang DS, E LL and Liu HC. Enhancement of periodontal tissue regeneration by transplantation of osteoprotegerin-engineered periodontal ligament stem cells. *Stem Cell Res Ther* 2015; 6: 22.
- [34] Menicanin D, Mrozik KM, Wada N, Marino V, Shi S, Bartold PM and Gronthos S. Periodontal-ligament-derived stem cells exhibit the capacity for long-term survival, self-renewal, and regeneration of multiple tissue types in vivo. *Stem Cells Dev* 2014; 23: 1001-1011.
- [35] Rethman MP and Harrel SK. Minimally invasive periodontal therapy: will periodontal therapy remain a technologic laggard? *J Periodontol* 2010; 81: 1390-1395.
- [36] Lindhe J and Nyman S. Scaling and granulation tissue removal in periodontal therapy. *J Clin Periodontol* 1985; 12: 374-388.